Journal of Inflammation Research

Dovepress
open access to scientific and medical research

Open Access Full Text Article

ORIGINAL RESEARCH

Electroacupuncture Modulates Microbial Phenylalanine Metabolism and Enhances the Intestinal Barrier Function to Alleviate Colitis in Mice

Lei Zhu[1,*], Ryan Au[2,*], Luming Dai[3,*], Yanan Li[2], Feng Xu[2], Yuan Cui[2], Jingyi Hu[1], Hong Shen[1]

[1]Digestive Disease Research Institute, Affiliated Hospital of Nanjing University of Chinese Medicine, City Nanjing, People's Republic of China; [2]First Clinical Medical College, Nanjing University of Chinese Medicine, City Nanjing, People's Republic of China; [3]Digestive Department, Affiliated Hospital of Nanjing University of Chinese Medicine, City Nanjing, People's Republic of China

*These authors contributed equally to this work

Correspondence: Hong Shen; Jingyi Hu, Digestive Disease Research Institute, Affiliated Hospital of Nanjing University of Chinese Medicine, City Nanjing, People's Republic of China, Email Shenhong999@njucm.edu.cn; hjytcm@163.com

Background: Electroacupuncture (EA) exerts beneficial effects on ulcerative colitis. However, its underlying mechanisms remain elusive. In this study, we investigated the impact of high and low-frequency EA at Zusanli (ST36) on the gut microbiota and metabolite profile in the dextran sulfate sodium (DSS)-induced colitis mouse model.

Methods: Colitis was established using DSS, and daily electroacupuncture at ST36 with varying frequencies was administered. Changes in body weight and fecal characteristics were monitored. Pro-inflammatory cytokines were detected, and the core molecule of intestinal barrier function were analyzed. The composition of intestinal flora was analyzed using 16S sRNA sequencing, while the changes of metabolites in colon tissue were detected by Ultra-performance liquid chromatography–tandem mass spectrometry (UPLC/MS/MS).

Results: Treatment with both high and low frequencies of EA at ST36 significantly ameliorated the symptoms of colitis, while also exerting systemic and local anti-inflammatory effect by downregulating the proinflammatory cytokines, iNOS and MPO. EA at ST36 enhanced the intestinal barrier by upregulating the expression of MUC2 and ZO-1. Furthermore, high-frequency EA at ST36 remarkably restored the gut microbial composition and diversity, as well as modulated the gut microbial metabolism of phenylalanine.

Conclusion: Our results suggest that EA treatment may alleviate colitis by reducing colon damage through gut microbiota-phenylalanine metabolism, which provides insight into EA's underlying mechanisms in the treatment of colitis.

Keywords: ulcerative colitis, electroacupuncture, gut microbiota, phenylalanine metabolism

Introduction

Ulcerative colitis (UC), characterized by chronic inflammation of the colon with damage to the intestinal barrier, has become a major worldwide public health concern.[1,2] While our understanding of its underlying mechanisms remains incomplete, environmental and genetic factors play a vital role in its development.[3,4] The intricate interplay between host physiology and gut microbiota serves as a central regulator within the intestinal ecosystem. The gut lumen harbors approximately 10,000 resident gut flora species, whose composition is influenced by various environmental cues. Dysbiosis, characterized by reduced diversity and perturbation in microbial composition, is widely recognized as a hallmark feature of colitis. Restoring microbial balance through fecal microbiota transplantation (FMT) or pharmaceutical intervention has proven efficacious in both clinical setting and animal models.[5–7] Non-pharmacological interventions like dietary therapy and acupuncture represent common clinical strategies for managing colitis symptoms;

Received: 11 June 2024
Accepted: 12 September 2024
Published: 14 October 2024

whereas pharmaceutical agents such as 5-aminosalicylic acid (5-ASA), glucocorticoids, and biologics carry potential risks for adverse effect.[8]

Originating from ancient Chinese medicine, acupuncture has been globally utilized for addressing a wide range of health issues. Electroacupuncture (EA), an innovative therapy derived from traditional acupuncture, is employed in the management of various condition such as inflammation, insomnia, depression, and Parkinson's disease.[9–12] Both clinical and animal research have shown that EA alleviates intestinal disorders, such as irritable bowel syndrome,[13] functional abdominal pain,[14] and inflammatory bowel disease (IBD).[15] The therapeutic efficacy of EA is frequency-dependent. Specifically, low-frequency EA (EA-L), defined as less than 30 hz, is associated with analgesic effects and enhanced local blood circulation, whereas high-frequency EA (EA-H), ranging from 30 hz to 1000 hz, exhibits anti-inflammatory properties and facilitates tissue repair.[16] Previous studies have indicated that treatment with varying frequencies of EA, particularly EA-H, can modulate macrophage polarization via the nucleotide-binding oligomerization domain, leucine-rich repeat and pyrin domain-containing 3 (NLRP3)/ interleukin-1 beta (IL-1β) and nuclear factor erythroid 2-related factor 2 (Nrf2)/heme oxygenase-1 (HO-1) pathways, thereby facilitating intestinal recovery in dextran sulfate sodium (DSS)-induced colitis.[17]

Given the role of gut microbiota in intestinal immunity, we hypothesized that EA may also influence gut flora and metabolites in the context of colitis. Interestingly, it has been reported that EA treatment (5 hz) can rebalance the composition of gut microbiota in 2,4,6-trinitrobenzene sulphonic acid (TNBS)-induced colitis.[18] Nevertheless, the precise mechanism by which EA operates within the gut microbial-metabolite pathway remains inadequately elucidated. Furthermore, EA-H treatment provides immunity regulation,[17] which suggests that EA-H may be more effective than EA-L at re-building the balance of microbial metabolism. Thus, we aimed to investigate the gut microbial regulation of different frequencies of EA on DSS-induced colitis to further uncovered the changes in gut microbial metabolites associated with EA treatment.

Materials and Methods

Reagents

DSS (36–50k MW, CAS:216011080) was obtained from MP Biomedicals (USA), and 5-ASA (CAT: A79809) was obtained from Sigma-Aldrich (USA). The cDNA synthesis Kit (CAT: R22-01) and qRT-PCR SYBR Green Kit (CAT: Q221-01) were obtained from Vazyme Biotech Co., Ltd. (Nanjing, China). Antibodies inducible nitric oxide synthase (iNOS, CAT: GB11119) and ZO-1 (CAT: GB111402) were purchased from Servicebio (Wuhan, China). Enzyme linked immunosorbent assay (ELISA) kit for myeloperoxidase (MPO) and pro-inflammatory cytokines, including IL-1β, IL-6, and tumor necrosis factor-alpha (TNF-α) were provided from Multi Sciences Biotech Co., Ltd. (Hangzhou, China).

Animals and Experimental Design

Five weeks-old male, specific-pathogen-free (SPF) C57BL/6J mice were purchased from Vital River Laboratory Animal Technology Co., Ltd. (Hangzhou, China) and housed in an SPF facility with a 12-h light/12-h dark cycle. The mice were randomly divided into the following five groups: Ctrl (n = 6), DSS (n = 8), DSS/EA-L (n = 8), DSS/EA-H (n = 8), and DSS/5-ASA (n = 8). All animals were acclimated for one week with free access to food and water prior to experimental procedures. Animal study and experimental procedures were approved by Animal Ethics Committee in Affiliated Hospital of Nanjing University of Traditional Chinese Medicine (Application Number: 2022DW–11–01) on May 10th, 2022.

As in previous studies,[19] acute colitis was induced by administering 2.5% DSS (w/v) to mice in the drinking water for a duration of 7 days, followed by subsequent period of 3 days during which autoclaved drinking water as provided. During the experiment, all mice were anesthetized with isoflurane at concentrations ranging from 0.5% to 1.5% until a surgical level of anesthesia was achieved, as confirmed by a negative pedal reflex test. The mice in Ctrl, DSS, and DSS/5-ASA groups were allowed to recover from anesthesia before being returned to their cages. The mice in DSS/EA-L and DSS/EA-H groups were received EA treatment. For EA treatment, the ST36 acupoint was accurately located on the hindlimbs, situated 4 mm inferior to the knee joint and approximately 2 mm lateral to the anterior tibial tuberosity. The surrounding area of ST36 was shaved, disinfected with 75% ethanol, and allowed to dry completely. Two sterile stainless

steel acupuncture needles were then inserted perpendicularly into ST36 at a depth of 3 mm. These needles were connected to an EA stimulator set to deliver an electrical current of 0.1 mA along with the specific frequency corresponding to each experimental group (DSS/EA-L group, 10 hz; DSS/EA-H group, 100 hz). The treatment was administered for a duration of 15 minutes, after which the mice were permitted to recover from anesthesia prior to being returned to their cages. One hour post-acupuncture treatment, the mice in the DSS/5-ASA group received 5-ASA (100 mg/kg) orally, while those in the other four groups were administered 0.2 mL of distilled water.

Disease Activity Index (DAI) Score

The DAI was scored every day. It was evaluated according previous study and it contained three parts: body weight loss (0, none; 1, < 5%; 2, 5–10%; 3, 10–20%; 4, >20%), stool consistency (0, normal; 2, loose stools; 4, diarrhea), and rectal bleeding (0, none; 2, slight bleeding; 4, gross bleeding). The DAI score was average of the three indexes.

Histopathological Analysis

The mice were humanely sacrificed by isoflurane overdose and cervical dislocation at day 11. Following measurement of the colon length, distal segments of colon tissue were fixed in 4% paraformaldehyde for 24 h, dehydrated, cleared, and embedded in paraffin wax. Colon tissue-containing paraffin blocks were sliced into 5 μm sections and transferred to glass slides for histological staining. Hematoxylin and eosin (H&E) and Alcian blue/periodic acid-Schiff (AB/PAS) staining were performed using kits from Wuhan Servicebio Technology Co., Ltd., according to the manufacturer's instructions. Stained specimens were observed under a light microscope.

Immunostaining of ZO-1 and iNOS

The paraffin sections on the slides were dewaxed with xylene, followed by rehydration using graded concentrations of alcohol. Endogenous peroxidase activity was eliminated blocked using 3% H_2O_2. After that, the slides were blocked with 5% goat serum for 30 min at 37°C. And the samples were incubated with primary antibody ZO-1 and iNOS for 12 h at 4°C. All the samples then were incubated with horseradish peroxidase-labelled secondary antibody (Cy5 conjugated Goat Anti-rabbit, GB27303, HRP conjugated Goat Anti-Rabbit, GB23303) for 1 h at 37°C. Images were observed using CaseViewer (Version 2.4; 3DHISTECH, Ltd).

RNA Extraction and Quantitative Real-Time Polymerase Chain Reaction (qRT-PCR)

Total RNA was extracted from colonic tissue samples using TRIzol™ Reagent (Invitrogen Corporation, USA) according to the manufacturer's instructions. The RNA purity and yield were evaluated by spectrophotometry. Complementary DNA was generated using the HiScript® III Reverse Transcription SuperMix system (Vazyme Biotech Co., Ltd., Nanjing, China). qRT-PCR was performed using the ChamQ SYBR qPCR Master Mix system (Vazyme Biotech Co., Ltd., Nanjing, China) and the LightCycler® 96 (Roche Diagnostics, Ltd., USA). β-actin was used as the housekeeping gene, and relative gene expression levels were calculated using the Livak method.[20] The primer sequences are listed in Table S1.

Enzyme-Linked Immunosorbent Assay (ELISA)

At day 11, blood samples were collected by retro-orbital bleeding after fasting for 12 hr. After centrifuged at 3000 g for 10 min, the supernatants were harvested as the serum samples. The levels of MPO and pro-inflammatory cytokines, including IL-1β, IL-6, and TNF-α, in serum were quantified using ELISA kits following the manufacturer's protocols.

DNA Extraction and Quantification of Bacteria in Ileocecal Contents

Genomic DNA was extracted from the ileocecal contents using the E.Z.N.A.® Stool DNA Kit (Omega Bio-tek, Inc., USA) according to the manufacturer's instructions. The DNA purity and concentration were assessed by spectrophotometry, and the DNA yield and quality were further confirmed by 1% agarose gel electrophoresis at 5 V/cm. The V3-V4 hypervariable region of genomic DNA was amplified in triplicate by PCR using primers 338F (5'-ACTCCTACGGGAGGCAGCAG-3') and 806R (5'-GGACTACHVGGGTWTCTAAT-3'). Then, the samples were pooled and run on a 2% agarose gel, and

amplicons from the correct band size were extracted and cleaned with the AxyPrep™ DNA Gel Extraction Kit (Axygen Scientific, Inc., USA). The final library concentration was measured using the QuantiFluor® dsDNA system (Promega Corporation, USA), according to the manufacturer's instructions. Purified amplicons were pooled in equimolar amounts and paired-end sequenced (2 × 300) on an Illumina MiSeq PE300 system (Illumina, Inc., USA) according to the standard protocols by Majorbio Bio-Pharm Technology Co., Ltd. (Shanghai, China).

Raw sequencing reads were demultiplexed and filtered using fastp v.0.23.0 and then merged using Fast Length Adjustment of SHort reads software v.1.2.11. Operational taxonomic units (OTUs) were clustered with the UPARSE function in USEARCH v.11.0.667, using a clustering threshold of 97% similarity. Chimeric sequences were identified and excluded. OTU sequences were then analyzed with RDP Classifier v.2.11 using the SILVA 16S rRNA database v.138.1, with a confidence threshold of 70%. Alpha diversity, beta diversity, community composition analysis, statistical analysis, and other calculations were performed at various taxonomic levels using the proprietary Majorbio Cloud platform (Shanghai Majorbio Bio-Pharm Technology Co., Ltd., China) according to standard protocols.

Metabolomic Analysis of Ileocecal Contents

Metabolomic analysis of ileocecal contents was performed by Shanghai Metabo-Profile Biotechnology Co., Ltd. The samples were prepared, followed by metabolite extraction and derivatization. Ultra-performance liquid chromatography–tandem mass spectrometry (UPLC/MS/MS) was performed to quantify all metabolites using the AcquityXevo TQ-S system (Waters™ Corporation, USA) coupled with a mass spectrometer. Targeted Metabolome Batch Quantification (TMBQ) software developed in-house by Shanghai Metabo-Profile Biotechnology Co., Ltd. was used to process the raw data by performing peak integration, calibration, and quantitation for each metabolite. Integrated Metabolomics Analysis Platform (iMAP) software, also developed in-house by the same company, was used for analysis of the metabolic data.

Statistical Analysis

All statistical analyses were performed on GraphPad Prism v. 9.0.0 (GraphPad Software, Inc., USA) using Analysis of Variance tests (ANOVA) for both paired comparisons and multiple comparisons. Statistical significance was defined as follows: * $P < 0.05$, ** $P < 0.01$, *** $P < 0.001$.

Results

EA Attenuates DSS-Induced Acute Colitis in Mice

To evaluate the beneficial impacts of EA on colitis, we established a chemical-induced mouse model by administering 2.5% DSS in drinking water for 7 days (Figure 1A–C). Following treatment with EA-L, EA-H, or 5-ASA, we assessed colitis indicators such as body weight loss, loose stool consistency, and fecal blood. As depicted in Figure 1D–G, both EA-L and EA-H treatment improved across these indicators, comparable to or exceeding those of 5-ASA. Additionally, the reduction in colon length post-DSS treatment was reversed following administration of EA-L, EA-H and 5-ASA (Figure 1H and I). Furthermore, H&E staining of the mucosa revealed that treatments with both EA-L and EA-H could effectively mitigate intestinal epithelial injury (Figure 1J). These findings validate the protective role of both high and low-frequency EAs against DSS-induced colitis.

EA Inhibits the Expression of Inflammatory Cytokines and Chemokines in the DSS-Induced Colitis

As colitis is a systemic inflammatory disease characterized by significant activation of the immune response,[21–23] we evaluated the effects of EA on inflammatory cytokine and chemokine expression in colonic tissue. The expression of pro-inflammatory cytokines (*Ifng, Nos2, Mpo, Il1b, Il6*, and *Tnfa*) and chemokines (*Cxcl9, Cxcl2, Ccl2*) was increased in the DSS group. However, they were reduced upon following EA treatment at both high and low frequencies, although the effect was more pronounced for EA-H (Figure 2A). The upregulated protein level of iNOS in colonic tissue was downregulated

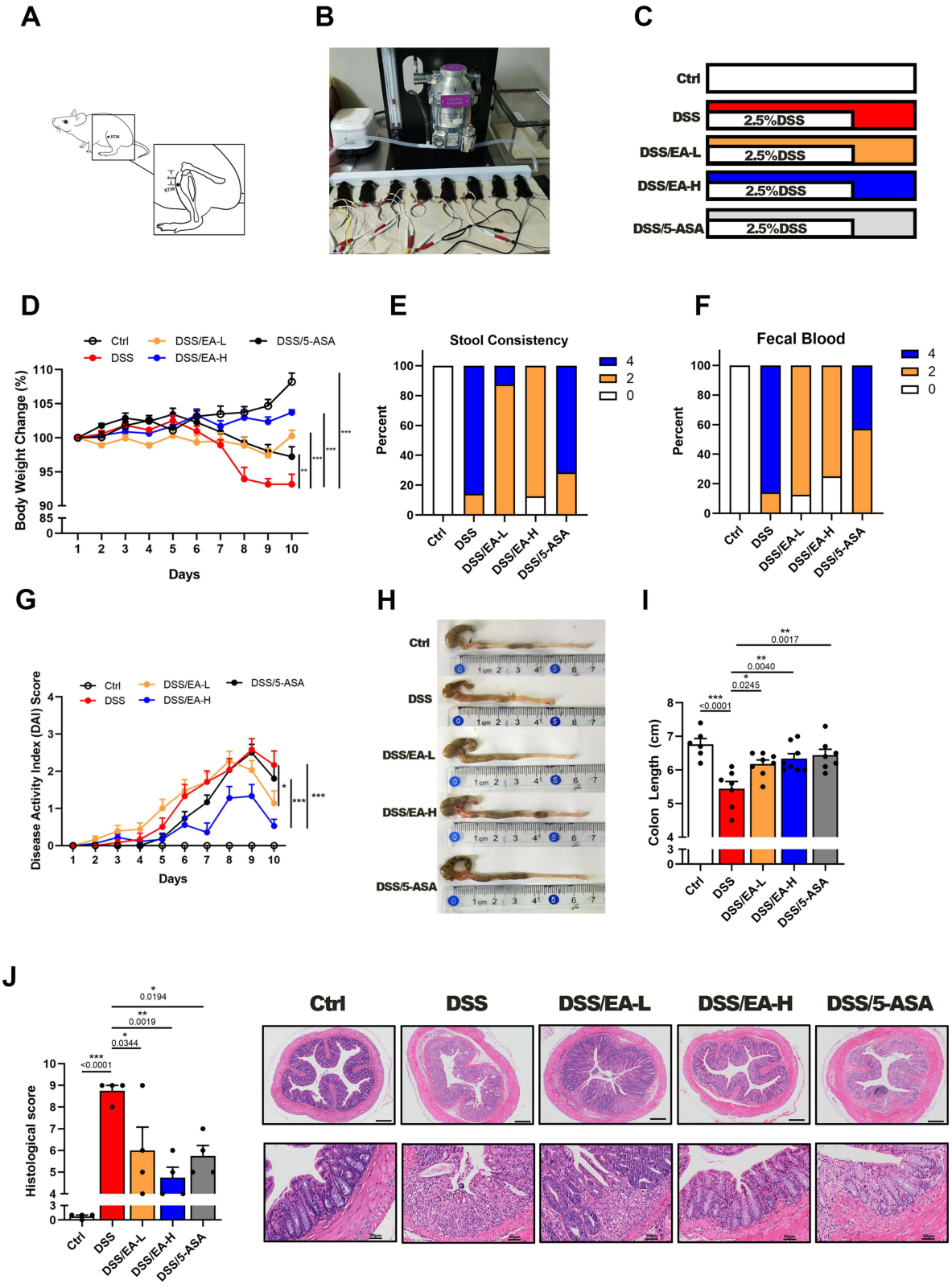

Figure 1 EA alleviates DSS-induced colitis in mice. (**A**) The location of the ST36 acupoint (also known as Zusanli). (**B**) Experimental set-up for treatment of mice using EA. (**C**) Experimental design for EA treatment. (**D**) Body weight change of mice after treatment with or without DSS (2.5% for 7 days) followed by EA-L (DSS/EA-L group, 10Hz), EA-H (DSS/EA-H group, 100Hz), or 5-ASA (dose 100 mg/kg), n = 6–8. (**E** and **F**) Percentage of stool consistency (**E**) and fecal blood (**F**) on day 10, n = 6–8. (**G**) Disease active index (DAI) score during colitis progression, n = 6–8. (**H** and **I**) Representative colonic images (**H**) and average length (**I**), n = 6–8. (**J**) Representative H&E staining images of colon (upper scar bar: 250 μm, bottom scar bar: 50 μm) and histological scores, n = 4. Data are expressed as the Mean ± SEM. * P < 0.05, ** P< 0.01, *** P< 0.001; one-way ANOVA with Tukey's post hoc analysis.

after EA treatment (Figure 2B). Furthermore, EA-H treatment significantly diminished the elevated serum levels of MPO, IL-1β, IL-6, and TNF-α in colitis, while EA-L treatment specifically reduced the levels of the latter three cytokines (Figure 2C). The data presented herein demonstrate that both low and high frequencies of EA treatment effectively mitigate the inflammatory response in the DSS-induced colitis model, as evidenced at both local and systemic levels.

EA Restores the Intestinal Barrier Integrity in the DSS-Induced Colitis

Colitis is typically characterized by compromised intestinal barrier function, the presence of lesions, a thinner mucosal barrier, and reduced expression of tight junction proteins.[24] Consequently, we assessed the impact of EA on the mRNA expression levels of barrier-related molecules including *Muc2, occludin*, and *Zo1*, as well as *Claudin2*, an indicator of intestinal permeability. Treatment with EA-L or EA-H reversed the decrease in *Muc2* and *occludin*, and EA-H additionally reversed the decrease in *Zo1* and the increase in *Claudin2* in the colonic tissues of DSS-treated mice (Figure 3A). Consistently, AB/PAS and immunohistochemical staining revealed a significant increase in the number of goblet cells and mucin production following EA treatment, accompanied by elevated expression of ZO-1 in colonic tissue (Figure 3B). Cumulatively, these findings suggest that EA mitigates DSS-induced impairment of the intestinal barrier.

EA Rebalances the Gut Microbiota in the DSS-Induced Colitis in Mice

Dysbiosis, with modification of the gut microbiota composition and downregulation of alpha diversity, is a typical characteristic of colitis.[25] As shown in Figure 4A and B, the Chao and Ace indices, which assess biodiversity, demonstrated a decline subsequent to DSS-induced colitis. However, EA-L treatment reversed the impact on the Chao index, while EA-H treatment reversed the effects on both indexes. By applying principal coordinate analysis (PCoA), we observed a clear demarcation between the Ctrl group and all DSS groups, indicating that EA treatment had minimal influence on the overall gut microbiota composition (Figure 4C). However, in Partial Least Squares Discriminant Analysis (PLS-DA) of inter-group similarity, the gut microbiota of the DSS/EA-L group exhibited similarity to that of the DSS group, whereas the DSS/EA-H group was demonstrated significant dissimilarity (Figure 4D). To further investigate this distinction, we assessed gut microbial communities at various hierarchical levels. Significantly divergent patterns were observed at phylum, family, and gene levels within the four experimental cohorts (Figure S1A, B and Figure 4E). To discern the distinct bacterial taxa between the DSS and DSS/EA-H groups at the gene level, we utilized STAMP analysis. The results revealed relatively elevated proportion of *norank_f_Lachnospiraceae, norank_f_UCG-010, Colidextribacter, norank_f_Christensenellaceae*, and *norank_f_Peptococcaceae* in the DSS/EA-H group, while *erysipelatoclostridium* and *clostridium_sensu_stricto_1* exhibited higher proportions in the DSS group (Figure 4F). Analysis by BugBase indicated that EA-H treatment significantly downregulated the abundance of potentially pathogenic microbiota (Figure 4G). Furthermore, the Kyoto Encyclopedia of Genes and Genomes (KEGG) pathway analysis using Phylogenetic Investigation of Communities by Reconstruction of Unobserved States 2 (PICRUSt2) revealed that EA-H treatment modulates metabolic pathways, particularly those related to cysteine and methionine metabolism, alanine, aspartate and glutamate metabolism, glycine, serine and threonine metabolism, lysine biosynthesis and phenylalanine (Phe), tyrosine and tryptophan biosynthesis (Figure 4H and I). The collective data suggests that EA-H reinstates the composition of gut microbiota and regulates amino acid metabolism in DSS-induced mice.

EA Rebalances Phenylalanine Metabolism in the Lumen of DSS-Treated Mice

Based on the aforementioned results, we employed untargeted metabolomics to investigate the impact of EA-H on the intestinal environment. Metabolite classification revealed that 21.33% of the compounds in fecal samples were fatty acids, 20.89% were amino acids, and 15.22% were bile acids (Figure 5A and B). Additionally, PLS-DA analysis unveiled distinctions in the metabolite profiles between the DSS and DSS/EA-H groups (Figure 5C). The relative quantities of metabolites were visualized using a heatmap, and the top 86 metabolites are shown in Figure 5D. The KEGG pathway analyses indicated that these differential metabolites were mainly involved in organic-acid-related metabolism, encompassing alpha-linolenic acid and linoleic acid metabolism, glutathione metabolism, arginine and proline metabolism, and phenylalanine and tyrosine metabolism (Figure 5E). Therefore, we analyzed the microbial metabolism of Phe (Figure 6A). The results showed that the concentration of each Phe metabolites was higher in DSS-treated mice

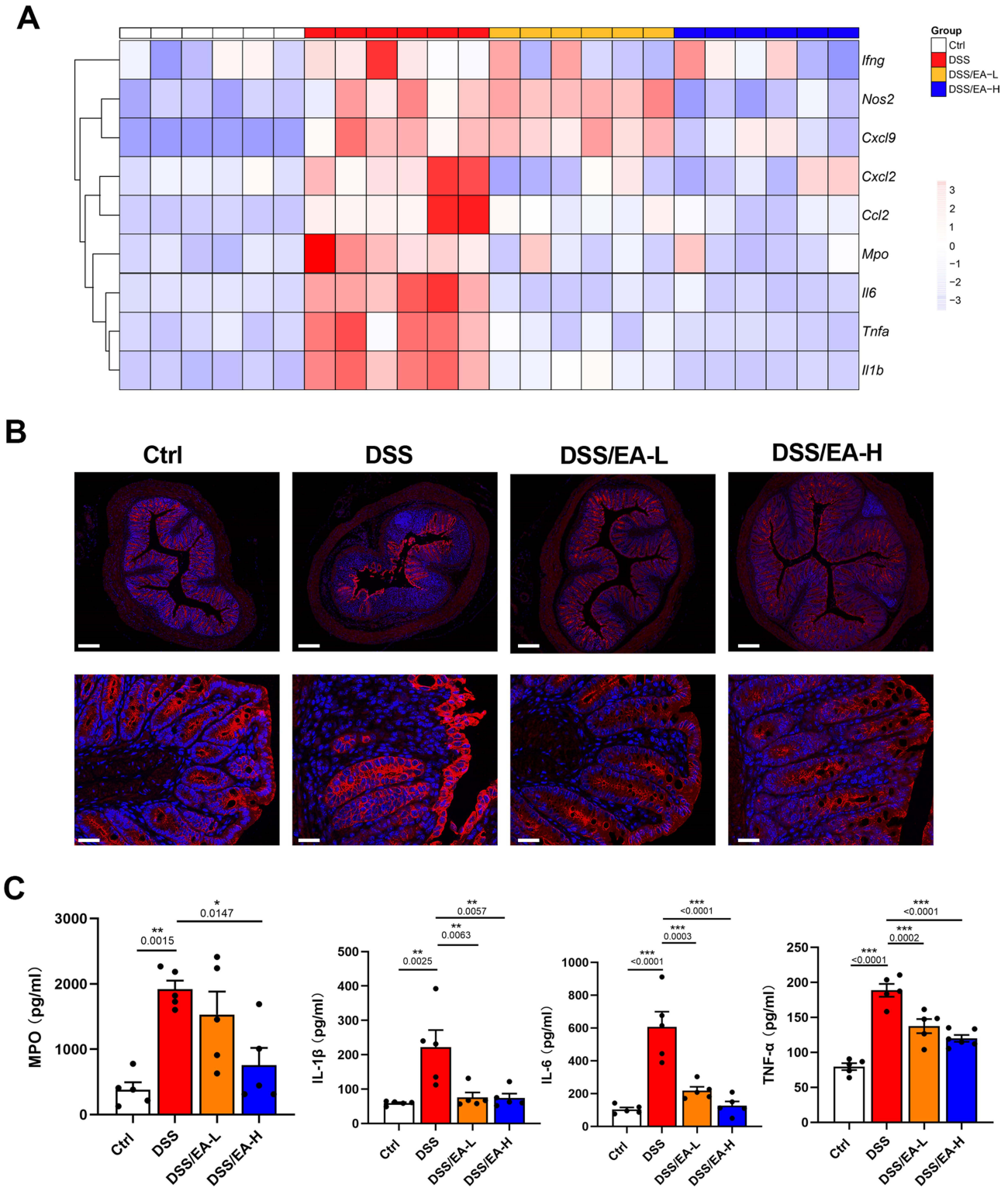

Figure 2 EA inhibits inflammatory cytokine and chemokine expression in the DSS-induced colitis in mice. (**A**) Heat map showing the relative mRNA expression of inflammatory cytokines (*Il1β, Il6, Infg*, and *Tnfa*), chemotactic factors (*Cxcl2, Cxcl9*, and *Ccl2), mpo*, and *Nos2* in the colonic tissue of Ctrl, DSS, DSS/EA-L, and DSS/EA-H groups of mice according to microarray analysis, n = 6. (**B**) Representative iNOS staining of colonic tissues of mice (upper scar bar: 250 μm, bottom scar bar: 50 μm). (**C**) ELISA of MPO, IL-1β, IL-6 and TNF-α levels in the serum of mice, n = 5. Data are expressed as the Mean ± SEM. *P < 0.05, **P< 0.01, ***P< 0.001; one-way ANOVA with Tukey's post hoc analysis.

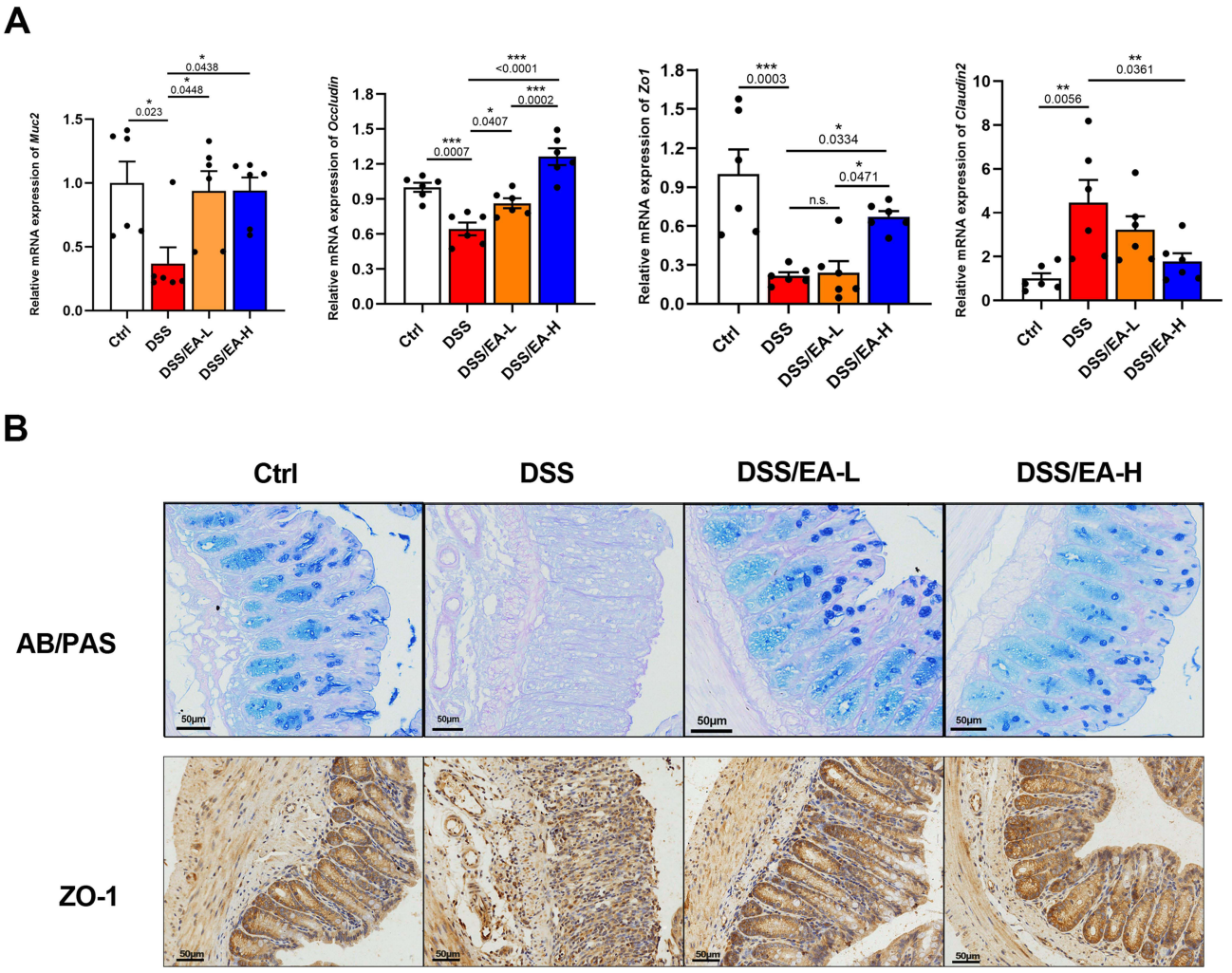

Figure 3 EA protects the intestinal barrier in DSS-induced colitis in mice. (**A**) The relative mRNA expression of *Muc2*, *Occluding*, *Zo1*, and *Claduin2* in colonic tissues of Ctrl, DSS, DSS/EA-L, and DSS/EA-H mice, n = 6. (**B**) Representative alcian blue/periodate Schiff (AB/PAS) and ZO-1 immunohistochemical staining of colonic tissue of mice (scar bar: 50 μm). Data are expressed as the Mean ± SEM. *P < 0.05, **P< 0.01, ***P< 0.001; one-way ANOVA with Tukey's post hoc analysis.

compared to normal mice, although only the differences in phenylpyruvic acid (PPyA) and phenyllactic acid (PPA) were statistically different. Additionally, EA-H treatment significantly downregulated the levels of these two metabolites (Figure 6A and B). Correlation analysis revealed a positive association between PPyA and *Romboutsia_ilealls*, Phe was positively associated with both *uncultured_organism_g_parasutterella* and *uncultured_bacterium_g_coriobacteriaceae UCG-002*. PPA was positively associated with *Romboutsia_ilealls* and *unclassified_g* _helicobacter, and negatively associated with *unclassified_g_lachnospiracea_NK4A136_group* (Figure 6C). Moreover, using MaAslin, a significant positive correlation of PPA with *unclassified_g_helicobacter* and a significant negative correlation of PPA with *unclassified_g_lachnospiracea_ NK4A136_ group* were observed (Figure 6D). These data indicate that EA-H rebuilds the microbial metabolism of Phe by modulating the microbial composition in DSS-treated mice.

Discussion

Current efforts have been focused on untangling the complex web of biological processes that underlie the development of colitis, including the identification of factors that prevent dysbiosis as a novel approach to developing potential new clinical therapies.[26] Non-pharmacological treatments are ideal choices for patients with UC because they tend to have fewer side effects.[27,28] These alternative approaches may include dietary modifications, lifestyle changes, and complementary therapies such as acupuncture or electroacupuncture. In this study, we have demonstrated

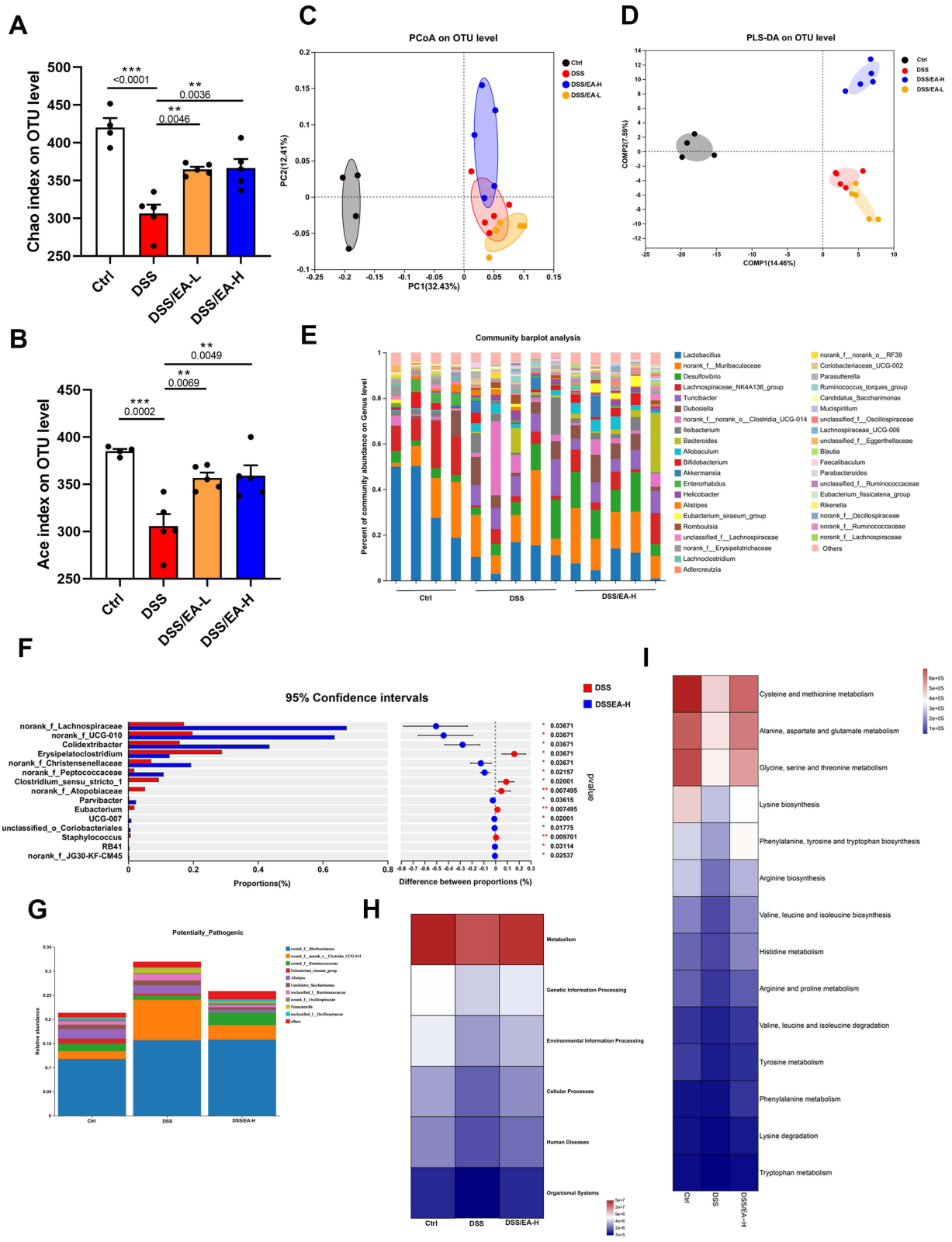

Figure 4 EA alters the composition of gut microbiota in DSS-treated mice. (**A** and **B**) α-diversity in gut microbiota of Ctrl, DSS, DSS/EA-L, and DSS/EA-H groups of mice according to the Chao and Ace indexes. (**C** and **D**) Principal coordinate analysis (PCoA) based on the unweighted UniFrac distance matrix and Partial Least Squares Discriminant Analysis (PLS-DA) at the OTU level. (**E** and **F**) Analysis of differences in microbial taxa at the gene level. (**G**) The relative abundance of potentially pathogenic microbiota based on BugBase function analysis. (**H** and **I**) Pathways at various levels exhibit distinct abundances among groups, as revealed by the Kyoto Encyclopedia of Genes and Genomes (KEGG) pathway analysis. Data are expressed as the Mean ± SEM. ** P< 0.01, *** P< 0.001; one-way ANOVA with Tukey's post hoc analysis.

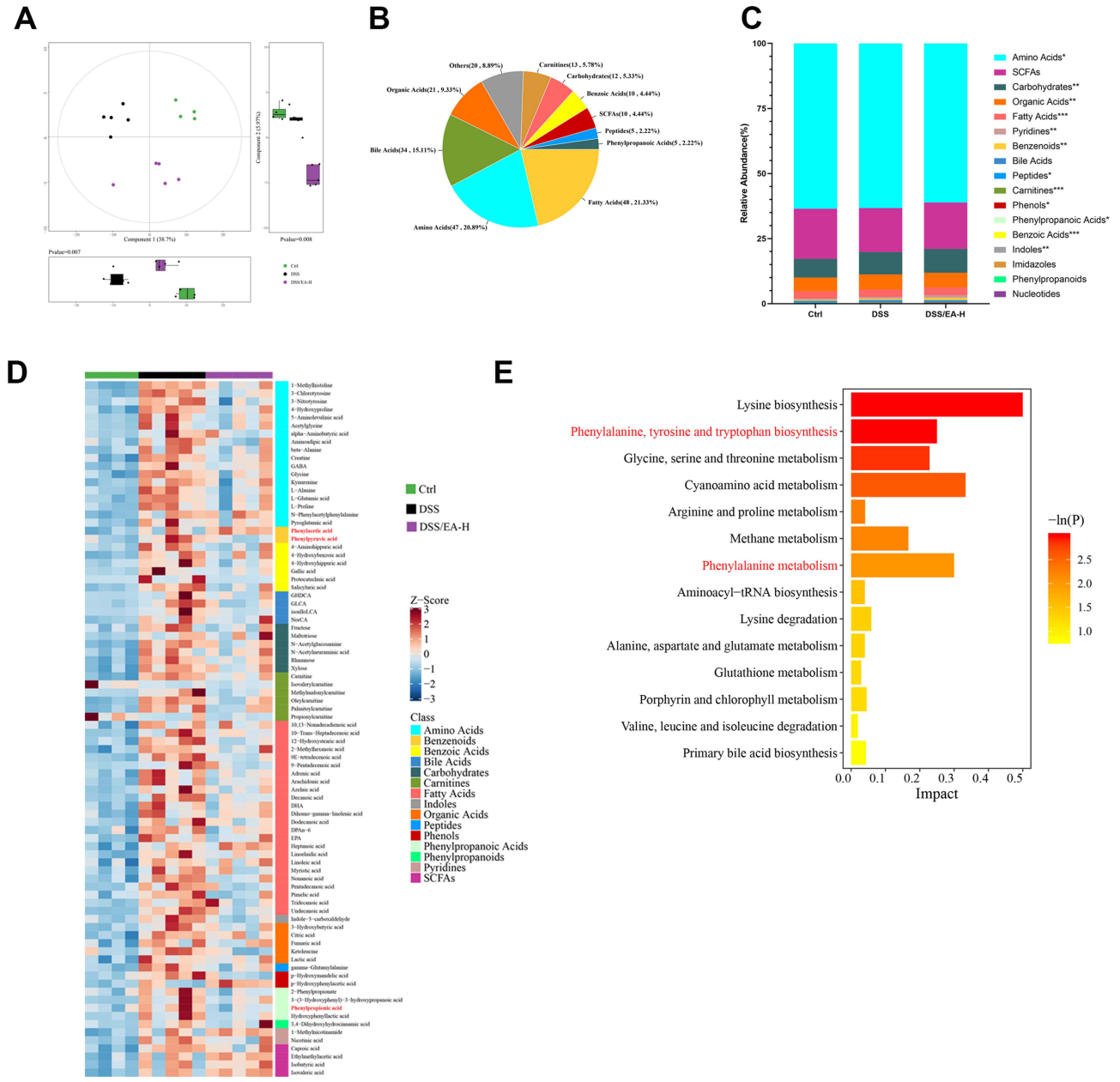

Figure 5 EA rebalances the metabolic profile in DSS-treated mice. (**A**) The fecal metabolomic profiles in Ctrl, DSS, and DSS/EA-H groups of mice were clustered using PLS-DA. (**B**) Total metabolome classification of compounds with differential metabolites. (**C**) The relative abundance of metabolites in each group of mice. (**D**) Heatmap of the levels of markedly altered metabolites. (**E**) KEGG pathway enrichment analysis according to the markedly altered metabolites. Data are expressed as the Mean ± SEM. *P < 0.05, **P< 0.01, ***P< 0.001; one-way ANOVA with Tukey's post hoc analysis.

that EA, a type of therapy that is administered non-pharmacologically at the ST36 acupoint using either high-frequency and low-frequency electrostimulation, alleviates DSS-induced colitis in mice. Notably, we demonstrated that EA-H significantly rebalances gut-microbiota Phe metabolism. Our results provide new insights into the benefits of EA and reveal an underlying metabolic mechanism associated with its therapeutic function.

Acupuncture has been a cornerstone of traditional Chinese medicine for centuries, and its integration into contemporary clinical practice is increasingly supported by emerging scientific data. The acupoint ST36, referred to as Zusanli in Chinese, is situated below the knee joint on the anterior aspect of the leg. This particular point has attracted attention not only due to its historical significance but also because of its physiological effects. Stimulation at ST36 has been demonstrated to modulate immune function across various diseases, including sepsis, diabetes mellitus, ischemic stroke,

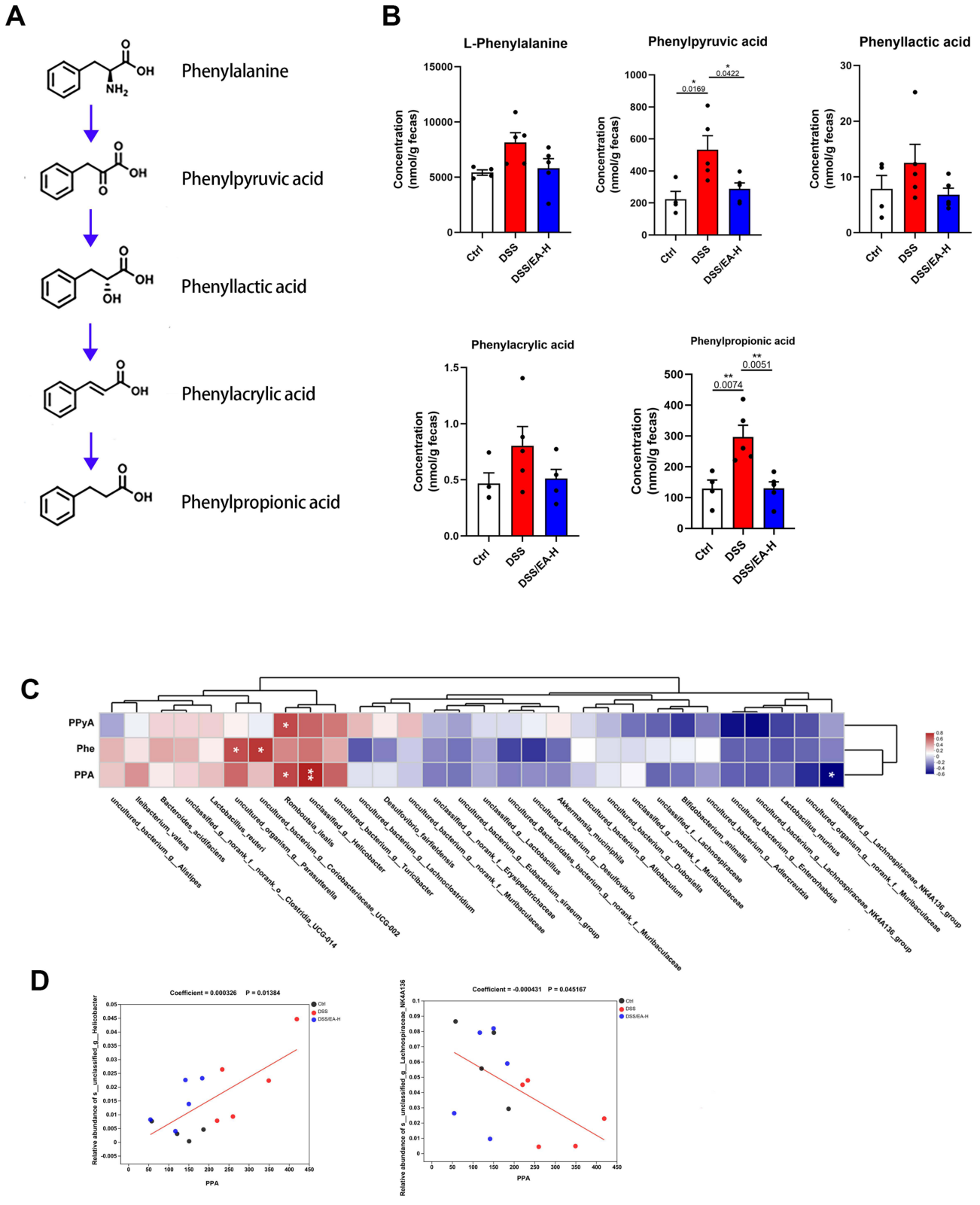

Figure 6 EA influences the metabolism of phenylalanine in DSS-treated mice. (**A**) Schematic diagram of Phenylalanine (Phe) metabolism. (**B**) The concentration of microbial metabolites of Phe in feces. (**C**) Correlation analysis between gut microbiota and Phe, phenylpyruvic acid (PPyA), and phenylpropionic acid (PPA). (**D**) MaAsLin analysis of gut microbiota and PPA. Data are expressed as the Mean ± SEM. *P < 0.05, ** P< 0.01; one-way ANOVA with Tukey's post hoc analysis.

and colitis.[29–31] Previous studies have reported that EA at ST36 or other acupoints has previously been shown to alleviate TNBS-induced colitis in rats and DSS-induced colitis in mice by regulating inflammatory cytokines.[18] However, it is important to note that while these studies have highlighted significant anti-inflammatory effects associated with EA treatment, they did not assess potential changes in gut microbiota composition or diversity resulting from such interventions. Moreover, existing literature suggests that high-frequency and low-frequency EA exhibit distinct functional impacts on biological systems.[9–12] These differences may stem from variations in neural activation patterns or downstream signaling pathways elicited by different frequencies. Consequently, we conducted an evaluation comparing both EA-H and EA-L specifically regarding their effects on models of colitis.

In this study, we observed that EA-H treatment in DSS-induced mice resulted in significant alterations to the microbiota, while the gut flora of DSS/EA-L mice exhibited a composition fundamentally akin to that of DSS mice. This suggests that EA-H may be a better choice for colitis treatment, which is consistent with its superior the ability to regulate the immune response.[17] To gain a more comprehensive understanding, we further identified the specific bacterial species influenced by EA-H. Our results demonstrate that *clostridium sensu stricto_1, norank_f_Atopobicea, Erysipelatoclostridium*, and *Eubacterium* are abundant in the gut flora of colitis mice, and *norank_f_Lachnospiraceae, norank_f_UCG-010, norank_f_Christensenellaceae*, and *norank_f_Peptococcaceae* are key microbiota associated with EA-H treatment mice. Moreover, BugBase analysis corroborated our findings by demonstrating that EA-H treatment markedly reduces the abundance of pathogenic microbiota typically associated with exacerbated colonic inflammation. The reduction in harmful microbes is crucial as it not only alleviates symptoms but also facilitates re-establishment of a balanced microbial community conducive to recovery. Collectively, these findings reinforce the potential of EA-H to mitigate colitis effects through mechanisms involving both immune modulation and restoration of a favorable colonic microbial environment.

Considering that alterations in gut microbiota composition frequently reflect functional transformations,[32–36] we performed a functional assessment utilizing PICRUSt prediction software, which revealed that amino acid metabolism was influenced by EA-H. The findings align with those of a prior study indicating that electroacupuncture at ST36 and SP6 (Sanyinjiao in Chinese) modulates levels of l-glutamine and gamma-aminobutyric acid in the hippocampi of colitis rats exhibiting anxiety and depression.[18] To substantiate our findings, we conducted an untargeted metabolic analysis utilizing UPLC/MS/MS. The results revealed significant alterations in the concentrations of amino acids, benzenoids, benzoic acids, and phenylpropanoic acids following EA-H treatment in colitis, with the metabolism of Phe and tyrosine (Tyr) ranking among the top ten changes. Consistently, two microbial metabolites of phenylalanine (PPyA and PPA) exhibited significant increases during colitis. The metabolism of phenylalanine, an aromatic amino acid, has been shown to be altered in IBD, with elevated concentrations reported in the feces of IBD patients.[37,38] In this study, we demonstrated that EA-H treatment significantly reduced levels of PPyA and PPA, thereby supporting the role of EA-H in modulating microbiota metabolism to alleviate colitis symptoms. These findings not only validate the therapeutic potential of EA for colitis but also provide mechanistic insights into the application of EA-H as a non-pharmacological strategy for disease amelioration.

Conclusion

EA at ST36, administered with high frequency, has been shown to inhibit colitis-related inflammation, restore the integrity of the mucosal barrier, and modulate intestinal microbiota along with its metabolic byproducts such as Phe, thereby alleviating DSS-induced colitis.

Ethics Statement

Animal experiments were performed at the Experimental Animal Center of the Affiliated Hospital of the Nanjing University of Chinese Medicine, strictly in accordance with the institution's ethical guidelines.

Acknowledgments

Lei Zhu, Ryan Au, and Luming Dai contributed equally to this work and share the first authorship.

Funding

This research was supported by Traditional Chinese Medicine Digestive Medicine Innovation Center of Jiangsu Province to H. S, High level key studies of traditional Chinese medicine of State Administration of Traditional Chinese Medicine to H. S, The third batch of leading talents in traditional Chinese medicine in Jiangsu Province to L. Z, the Youth talents project of Jiangsu Administration of Traditional Chinese Medicine (grant number QN202106 to J.H), Outstanding young Doctor training program of Jiangsu Provincial Hospital (grant number 2023QB0132 to J.H).

Disclosure

The authors declare that they have no conflict of interest.

References

1. Kaplan G, Ng S. Understanding and preventing the global increase of inflammatory bowel disease. *Gastroenterology*. 2017;152(2):313–321.e2. doi:10.1053/j.gastro.2016.10.020
2. Kaplan G. The global burden of IBD: from 2015 to 2025. *Nat Rev Gastroenterol Hepatol*. 2015;12(12):720–727. doi:10.1038/nrgastro.2015.150
3. Ananthakrishnan A, Bernstein C, Iliopoulos D, et al. Environmental triggers in IBD: a review of progress and evidence. *Nat Rev Gastroenterol Hepatol*. 2018;15(1):39–49. doi:10.1038/nrgastro.2017.136
4. Molodecky N, Panaccione R, Ghosh S, Barkema H, Kaplan G. Challenges associated with identifying the environmental determinants of the inflammatory bowel diseases. *Inflamm. Bowel Dis*. 2011;17(8):1792–1799. doi:10.1002/ibd.21511
5. Haifer C, Luu L, Paramsothy S, Borody T, Leong R, Kaakoush N. Microbial determinants of effective donors in faecal microbiota transplantation for UC. *Gut*. 2022. doi:10.1136/gutjnl-2022-327742
6. Moayyedi P, Surette M, Kim P, et al. Fecal microbiota transplantation induces remission in patients with active ulcerative colitis in a randomized controlled trial. *Gastroenterology*. 2015;149(1):102–109.e6. doi:10.1053/j.gastro.2015.04.001
7. Song M, Chan A, Sun J. Influence of the gut microbiome, diet, and environment on risk of colorectal cancer. *Gastroenterology*. 2020;158 (2):322–340. doi:10.1053/j.gastro.2019.06.048
8. Ryan C, Harisha UK, Wenwen Z, Shashi A, Walter R. Impact of concomitant 5-aminosalicylic acid therapy on vedolizumab efficacy and safety in inflammatory bowel disease: post hoc analyses of clinical trial Data. *J Crohn Colit*. 2023;17(12):1949–1961. doi:10.1093/ecco-jcc/jjad113
9. Ulett G, Han S, Han J. Electroacupuncture: mechanisms and clinical application. *Biological Psychiatry*. 1998;44(2):129–138. doi:10.1016/s0006-3223(97)00394-6
10. Zou R, Zhang H, Zhang T. Comparative study on treatment of acute gouty arthritis by electroacupuncture with different frequency. *Chin J Integrat Med*. 2006;12(3):212–214. doi:10.1007/bf02836525
11. Kim H, Uh D, Yoon S, et al. Low-frequency electroacupuncture suppresses carrageenan-induced paw inflammation in mice via sympathetic post-ganglionic neurons, while high-frequency EA suppression is mediated by the sympathoadrenal medullary axis. *Brain Res Bull*. 2008;75 (5):698–705. doi:10.1016/j.brainresbull.2007.11.015
12. Wang K, Zhang R, He F, et al. Electroacupuncture frequency-related transcriptional response in rat arcuate nucleus revealed region-distinctive changes in response to low- and high-frequency electroacupuncture. *J Neurosci Res*. 2012;90(7):1464–1473. doi:10.1002/jnr.23028
13. Pei L, Geng H, Guo J, et al. Effect of acupuncture in patients with irritable bowel syndrome: a randomized controlled trial. *Mayo Clin Proceed*. 2020;95(8):1671–1683. doi:10.1016/j.mayocp.2020.01.042
14. Hong S, Ding S, Wu F, et al. Efficacy and safety of manual acupuncture manipulations with different frequencies on epigastric pain syndrome (EPS) in functional dyspepsia (FD) patients: study protocol for a randomized controlled trial. *Trials*. 2017;18(1):102. doi:10.1186/s13063-017-1845-3
15. Horta D, Lira A, Sanchez-Lloansi M, et al. A prospective pilot randomized study: electroacupuncture vs. sham procedure for the treatment of fatigue in patients with quiescent inflammatory bowel disease. *Inflammatory Bowel Diseases*. 2020;26(3):484–492. doi:10.1093/ibd/izz091
16. Guo Y. *Experimental Acupuncture Science*. China Press of Traditional Chinese Medicine; 2008.
17. Song S, An J, Li Y, Liu S. Electroacupuncture at ST-36 ameliorates DSS-induced acute colitis via regulating macrophage polarization induced by suppressing NLRP3/IL-1β and promoting Nrf2/HO-1. *Molecular Immunology*. 2019;106:143–152. doi:10.1016/j.molimm.2018.12.023
18. Zhou F, Jiang H, Kong N, et al. Electroacupuncture attenuated anxiety and depression-like behavior via inhibition of hippocampal inflammatory response and metabolic disorders in TNBS-Induced IBD rats. *Oxidative Medicine and Cellular Longevity*. 2022;2022:8295580. doi:10.1155/2022/8295580
19. Hu J, Huang H, Che Y, et al. Qingchang Huashi Formula attenuates DSS-induced colitis in mice by restoring gut microbiota-metabolism homeostasis and goblet cell function. *J Ethnopharmacol*. 2021;266:113394. doi:10.1016/j.jep.2020.113394
20. Livak K, Schmittgen T. Analysis of relative gene expression data using real-time quantitative PCR and the 2(-Delta Delta C(T)) Method. *Methods*. 2001;25(4):402–408. doi:10.1006/meth.2001.1262
21. Ungaro R, Mehandru S, Allen P, Peyrin-Biroulet L, Colombel J-F. Colombel, Ulcerative colitis. *Lancet*. 2017;389(10080):1756–1770. doi:10.1016/s0140-6736(16)32126-2
22. Ordás I, Eckmann L, Talamini M, Baumgart DC, Sandborn WJ. Ulcerative colitis. *Nat Rev Dis Prim*. 2020;6(1):73. doi:10.1038/s41572-020-00215-4
23. Ulcerative colitis. Nature reviews. *Disease Primers*. 2020;6(1):73. doi:10.1038/s41572-020-00215-4
24. Neurath M, Vieth MJG. Different levels of healing in inflammatory bowel diseases: mucosal, histological, transmural, barrier and complete healing. Gut. 2023;72(11):2164–2183. doi:10.1136/gutjnl-2023-329964
25. Karlsen TH. Hepatology, The microbiota and the gut-liver axis in primary sclerosing cholangitis. *Gut*. 2023;20(3):135–154. doi:10.1038/s41575-022-00690-y

26. Liu S, Zhao W, Lan P, Mou X. The microbiome in inflammatory bowel diseases: from pathogenesis to therapy. *Protein & Cell*. 2020. doi:10.1007/s13238-020-00745-3
27. Haskey N, Estaki M, Ye J, et al. A Mediterranean Diet Pattern improves intestinal inflammation concomitant with reshaping of the bacteriome in ulcerative colitis: a randomized controlled trial. *Journal of Crohn's & Colitis*. 2023;17:1569–1578. doi:10.1093/ecco-jcc/jjad073
28. Fritsch J, Garces L, Quintero M, et al. Low-fat, high-fiber diet reduces markers of inflammation and dysbiosis and improves quality of life in patients with ulcerative colitis. *Clin Gastroenterol Hepatol*. 2021;19(6):1189–1199.e30. doi:10.1016/j.cgh.2020.05.026
29. Hu X, Song L, Zhang Z, et al. Electroacupuncture at ST25 corrected gut microbial dysbiosis and SNpc lipid peroxidation in Parkinson's disease rats. *Frontiers in Microbiology*. 2024;15:1358525. doi:10.3389/fmicb.2024.1358525
30. Cao L, Zhou S, Li J, Chen K, Xue X, Yi W. Effects of electroacupuncture on intestinal microflora and plasma metabolites in an insulin-resistant mouse model of type 2 diabetes mellitus. *Acupuncture in Medicine*. 2024;42(2):76–86. doi:10.1177/09645284231207871
31. Xu H, Wen Q, Hu H, et al. Electroacupuncture at ST36 modulates the intestinal microecology and may help repair the intestinal barrier in the rat model of severe acute pancreatitis. *Microbial Biotechnology*. 2024;17(2):e14401. doi:10.1111/1751-7915.14401
32. Flint H, Scott K, Louis P, Duncan S. The role of the gut microbiota in nutrition and health. *Nat Rev Gastroenterol Hepatol*. 2012;9(10):577–589. doi:10.1038/nrgastro.2012.156
33. Agus A, Planchais J, Sokol H. Gut microbiota regulation of tryptophan metabolism in health and disease. *Cell Host Microbe*. 2018;23(6):716–724. doi:10.1016/j.chom.2018.05.003
34. Shin JH, Lee YK, Shon WJ, et al. Gut microorganisms and their metabolites modulate the severity of acute colitis in a tryptophan metabolism-dependent manner. *Eur J Nutr*. 2020. doi:10.1007/s00394-020-02194-4
35. Duboc H, Rajca S, Rainteau D. Connecting dysbiosis, bile-acid dysmetabolism and gut inflammation in inflammatory bowel diseases. *Gut*. 2013;62(4):531–539. doi:10.1136/gutjnl-2012-302578
36. Singh V, San Yeoh B, Walker RE, et al. Microbiota fermentation-NLRP3 axis shapes the impact of dietary fibres on intestinal inflammation. *Gut*. 2019;2019:1.
37. Papada E, Forbes A, Amerikanou C, et al. Antioxidative efficacy of a *Pistacia lentiscus* supplement and its effect on the plasma amino acid profile in inflammatory bowel disease: a randomised, double-blind, placebo-controlled trial. *Nutrients*. 2018;10(11). doi:10.3390/nu10111779
38. Jagt J, Verburgt C, de Vries R, et al. Faecal metabolomics in paediatric inflammatory bowel disease: a systematic review. *J Crohn's Colitis*. 2022;16(11):1777–1790. doi:10.1093/ecco-jcc/jjac079